24th INTERNATIONAL CONGRESS ON SOUND AND VIBRATION
23–27 July 2017, London

CLUSTERING INVERSE BEAMFORMING FOR VEHICLES NVH

Claudio Colangeli, Karl Janssens

Siemens Industry Software NV, Leuven, BE
email: claudio.colangeli@siemens.com

Paolo Chiariotti and Paolo Castellini

Università Politecnica delle Marche, Dip. di Ingegneria Industriale e Scienze Matematiche, Ancona, IT.

Clustering Inverse Beamforming is an array-based acoustic imaging technique to solve inverse problems formulated by discretizing the source region into elementary equivalent sources. It is based on a statistical processing of multiple realizations of the acoustic image, related to the investigated source region, iteratively obtained solving the corresponding inverse problem on different clusters of microphones, taken from the same microphones array. The result of such statistical processing is stored in the so-called "clustering mask matrix". This function is defined, in the source region, where it is interpretable as the confidence level of finding a physical source in each location within the domain. The inner statistical nature of such approach prevents the occurrence of numerical issues related to the solution of the inverse problem. It allows accurate localization and optimal quantification by enabling to focus on those sub-regions most likely to be the location of physical sources. Moreover, if combined with Principal Component Analysis, the method provides a robust criterion for uncorrelated noise source separation with no need of reference sensors in the proximity of the investigated object. Clustering Inverse Beamforming is applicable to exterior as well as to interior acoustic imaging problems. It does not require any special geometrical configuration of the microphones array. The technique is presented both on numerical simulations and on experiments related to vehicles NVH applications.

Keywords: acoustic imaging, beamforming, inverse methods, NVH.

1. Introduction

Experimental acoustic imaging methods such as beamforming and Near-field Acoustic Holography are used in vehicle noise and vibration studies because they are capable of identifying the noise sources contributing to the overall noise perceived inside and outside the cabin. However, these techniques are often relegated to the troubleshooting phase, thus requiring additional experiments for more detailed NVH analyses. It is therefore desirable that such methods evolve towards more refined solutions capable of providing a wider and more detailed information.

This paper introduces a new approach for improving the potential of inverse acoustic imaging methods and discusses its use on NVH applications. The idea of the method is to obtain additional statistical information from the performed acoustic imaging experiment, to be combined with an Equivalent Source Method (ESM) solution. The final result is enhanced in terms of localization and dynamic range. Moreover, it will be shown that this method, called Clustering Inverse Beamforming (CIB), allows absolute source quantification and identification of correlated and uncorrelated source distributions, without any help from any additional reference sensor.

CIB is therefore a processing technique for improving ESM results. The crucial aspect in the formulation of the clustering approach is in the statistical nature of the data that are manipulated. Such vision has been inspired by the so-called average beamforming method proposed by Castellini and Sassaroli in [1]. The concept of combining different areas of a microphone array has been exploited

also in other ways in literature. Guidati and Sottek in [2] discuss pros and cons of the use of a modular microphones array adopting a "flexible" geometry allowing to adjust the aperture of the array to the targeted acoustic scene or to combine results of arrays with larger and smaller aperture. Elias proposes in [3] a so-called multiplicative beamforming (MBF), whose main purpose is to enhance the SSL solution by suppressing the unwanted effects of side-lobes of a direct beamformer. In its original formulation it is conceived for cross/star shaped arrays and requires the use of direct beamforming methods [4]. The extension of the idea towards interior applications have also been proposed [5].

Contrarily to the reported cases, which share the characteristics of being deterministic and of exploiting direct beamforming methods, CIB is an inverse method that combines, in a statistical formulation, the results of an ESM algorithm on clusters of data belonging to the same microphones array. The probabilistic interpretation of the acoustic imaging data makes this method highly compatible with inverse methods grounded on a Bayesian vision of the studied acoustic problem [6].

CIB was presented for the first time in [7] and then extended in [8, 9]. The inner statistical nature of CIB makes it versatile - because it can be applied using any kind of array shape and geometry - and general because it can be applied in exterior as well as interior applications without any change to the processing strategy. These characteristics make this method appealing for advanced applications to source identification in the frame of vehicles NVH.

The formulation of the method will be reported in section 2. The ability of the method of dealing with uncorrelated as well as with correlated sources will be proven in section 3 through an application on simulated data. The method will be then applied on experimental data acquired during an in-door pass-by noise test of an electric vehicle (section 4). CIB's effectiveness and potential future avenues will be finally discussed in section 5.

2. Theory

CIB relies on multiple realizations of an inverse acoustic problem solution obtained thorugh an ESM. Among the many options, in this paper the Generalized Inverse Beamforming (GIBF [9, 10]) method will be used. The GIBF algorithm works in frequency domain and starts with the computation of the Cross-Spectral Matrix (CSM) of the microphone array signals. The CSM is an M×M matrix - M is the number of microphones in the array - whose elements consist in the cross-spectra between the signals of each pair of microphones of the array. The main diagonal of the CSM contains the Auto-Power Spectra (APS) of the signals of each microphone. The eigenvalue decomposition of the microphone array CSM (C_M)

$$C_M = ESE^H \tag{1}$$

makes it possible to decompose the acoustic field at the array plane in eigenmodes (Eq. (1)). E and S represent, respectively, the eigenvectors and the eigenvalues matrices of size M×M. They are composed, respectively, by:

- $\underline{e}^{(i)}$, column vector of E, whose elements are: $e^{(i)}{}_m$;
- s_i, diagonal elements of S, eigenvalues of C_M.

The symbol "^{H}" indicates the conjugate (or Hermitian) transpose. Each eigenmode corresponds to an uncorrelated source distribution. it is recommended to calculate the CSM taking, as rule of thumb, at least 10×M averages in order to obtain a correct estimation of the APS of the uncorrelated source distributions active in the field through eigenvalue decomposition. A theoretical explanation of this assumption is given in [11].

$$P = [\ \underline{p}^{(1)} \quad ... \quad \underline{p}^{(i)} \quad ..... \quad \underline{p}^{(L)} \quad ... \quad \underline{p}^{(M)}\ ] = E\sqrt{S} \tag{2}$$

In Eq. (2), L represents the number of not negligible eigenmodes (also called: *principal components*) of C_M. Physically, each distribution $\underline{p}^{(i)}$ at the array plane is the result of the sound propagation of the corresponding source distribution $\underline{a}^{(i)}$ located at the calculation plane.

The eigenmodes decomposition of the CSM is also convenient because it allows to theretically compute the acoustic power (W_i) of each uncorrelated source distribution:

$$W_i = \frac{\rho}{8\pi c}\frac{s_i - s_M}{\rho^2 M R_r}. \tag{3}$$

Assuming a radiation model suitable for monopole sources in free field conditions

$$\{A\}_{m,n} = \frac{e^{-ikr_{mn}}}{4\pi r_{mn}} \tag{4}$$

- r_{mn} being the distance between the mth of the M microphones and the nth of the N scan points composing the calculation plane - the radiation problem can be formulated as follows:

$$\underline{a}^{(i)} \quad s.t. \quad A\underline{a}^{(i)} = \underline{p}^{(i)} \quad \forall i = 1,...,L. \tag{5}$$

The inverse problem is solved through the pseudo-inverse of the radiation matrix *A*. The radiation matrix *A* is generally ill-conditioned, thus a regularization strategy is required. The Tikhonov's approach is exploited for the inversion. Regularization is obtained by introducing a parameter (λ^2) in the generalized inversion as shown in Eq. (6) where *I* is the identity matrix of size M×M.

$$\underline{a}^{(i)} = A^H (AA^H + \lambda^2 I)^{-1} \underline{p}^{(i)} \tag{6}$$

Among the available criteria ([12] and references therein) to identify the regularization parameter, in this study we have chosen the *quasi-optimality function* method on the basis of previous studies [11].

Suzuki [10] proposed to use an iterative process for improving the identification task. He suggested to solve Eq. (6) iteratively for a fixed number of times, updating the problem at each iteration and discarding, from the equivalent source solution vector $\underline{a}^{(i),\,k=*}$, the scan points showing the weakest amplitude (thus the weakest strength). Discarding the redundant unknowns (therefore reducing numerical instabilities) allows for better posing the inverse problem, leading to a more accurate identification of the source distributions. The same approach is adopted in this formulation.

The clustering approach is based on the principle that the solution of an inverse acoustic imaging problem is strongly dependent on the radiation matrix *A* considered. Indeed, by selecting only certain rows of *A*, i.e. considering a subset - cluster - of microphones among those constituting the whole array, the mathematical formulation of the problem changes, while the physical problem remains obviously the same. The regularization strategy and the iterative solution of GIBF will act differently depending on the radiation matrix considered: in this way, any numerical instability that give rise to ghost sources will vary, while the actual sources will be constantly identified. This evidence is exploited performing the GIBF iterative process N_c times on N_c different clusters composed of N_m microphones. The set of GIBF solutions obtained in this way ($\tilde{\underline{a}}^{(i)}{}_c$, c=1, … , N_c) for each one of the main eigenmodes (or for the overall acoustic field if $\underline{p} = \Sigma_{(i)}\underline{p}^{(i)}$ is used instead of $\underline{p}^{(i)}$), will be processed in order to obtain a so-called "*clustering mask matrix*". This matrix will be exploited to finally obtain an enhanced acoustic image. The clusters are more effective if the distribution of their microphones is as much homogeneous as possible with respect to the area of the full array. The statistical manipulation of the set of solutions $\tilde{\underline{a}}^{(i)}{}_c$ yields two functions: the normalized *mean matrix* and the normalized *occurrences matrix*. The first one is defined as the averaged map, per eigenmodes, of the N_c realizations of the solutions obtained per clusters, the second matrix emphasizes the effect of the averaging process for providing statistical consistency [9]. This latter effect is obtained adopting the function ε which returns value 1 if its argument is non-zero, 0 otherwise:

$$\varepsilon(\tilde{\underline{a}}^{(i)}{}_c) \quad s.t. \quad \begin{cases} \varepsilon(\tilde{\underline{a}}^{(i)}{}_c(n) = 0) = 0 \\ \varepsilon(\tilde{\underline{a}}^{(i)}{}_c(n) \neq 0) = 1 \end{cases} \quad \forall n = 1,...,N. \tag{7}$$

The two matrices are then combined in the *clustering mask matrix*, $\gamma^{(i)}$, in which the *mean matrix* and the *occurrences matrices* are Hadamard multiplied:

$$\gamma^{(i)} = \overbrace{\frac{\sum_{c=1}^{N_c} \tilde{\underline{a}}^{(i)}{}_c}{\max\left(\sum_{c=1}^{N_c} \tilde{\underline{a}}^{(i)}{}_c\right)}}^{Mean\ matrix} \cdot \overbrace{\frac{\sum_{c=1}^{N_c} \varepsilon(\tilde{\underline{a}}^{(i)}{}_c)}{\max\left(\sum_{c=1}^{N_c} \varepsilon(\tilde{\underline{a}}^{(i)}{}_c)\right)}}^{Occurrences\ matrix}. \tag{8}$$

CIB obtains the final solution as a function of the inverse acoustic image $Y(A,\underline{p}^{(i)})$, calculated using the full set of microphones information, and the mask matrix $\gamma^{(i)}$ obtained through Eq. (8). This approach (Fig. 1 *(a)*) is formalized in the expression:

$$\underline{a}^{(i)} = \mathrm{Y}(A, \underline{p}, \gamma^{(i)}). \tag{9}$$

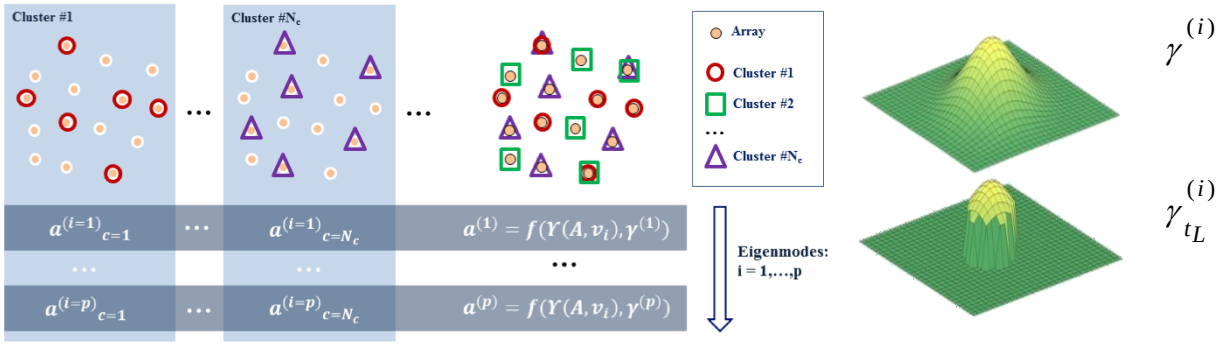

(a) *(b)*

Figure 1: *(a)* Description of the Clustering Inverse Beamforming principle: the solution is obtained (per eigenmodes) in multiple realizations adopting each time a different cluster (sub-set) of microphones. The final solution is optimized on the basis of the statistical information added by this processing. *(b)* Selecting a confidence level is equivalent to consider only the regions of those scan points in which the clustering mask matrix value is above a wanted threshold t_L.

The mask matrix $\gamma^{(i)}(n)$ is interpreted as a function that expresses the probability that the nth equivalent source in the scan grid corresponds to a physical source distribution in the acoustic image. This probability information is obtained *a posteriori* interpreting the equivalent sources corresponding to the values of the mask matrix closer to 1 as the most likely source distribution representative of the investigated acoustic scene. This suggests, as formalized in Eq. (10), to select in the optimized inverse problem only those equivalent sources locations in the scan grid assuming mask matrix values above a wanted threshold t_L called confidence level (Fig. 1 *(b)*).

$$\underline{a}^{(i)} = \mathrm{Y}\left(\{A\}_{M,f\left(\gamma^{(i)}_{t_L}\right)}, \underline{p}^{(i)}\right) \tag{10}$$

This approach has the advantage of adopting the mask matrix for improving both the localization, selecting the equivalent sources close to its local maxima, and the quantification task, computing the strength of the equivalent sources only in the regions where a physical source is most likely expected.

3. Numerical simulation of uncorrelated and correlated sources

In the simulated scenario, introduced in this section to prove CIB capability of accurate localization and ranking of correlated and uncorrelated sources, an array of 43 randomly distributed microphones is placed 0.6 m far from the sources plane and the two monopole sources (S#1 and S#2) are located as in Fig. 2 *(a)*. In one case the two sources emit two band limited (1-10 kHz) uncorrelated

white noise signals. S#2 is generated with higher strength in order to be systematically assigned to the first eigenmode of the correspondent CSM. In a second case, the two ideal monopolar sources will emit the same band limited white noise signal in order to simulate perfect correlation. In the first case the sources are espected to be assigned to two different eigenmodes, while in the latter case they are supposed to be identified as belonging to one eigenmode of the CSM.

Where not differently specified, the acoustic images will be reported with dynamic range of 40 dB and the mask matrices will be represented using a linear scale ranging from 0 to 1 (Fig. 2 *(b-c)*).

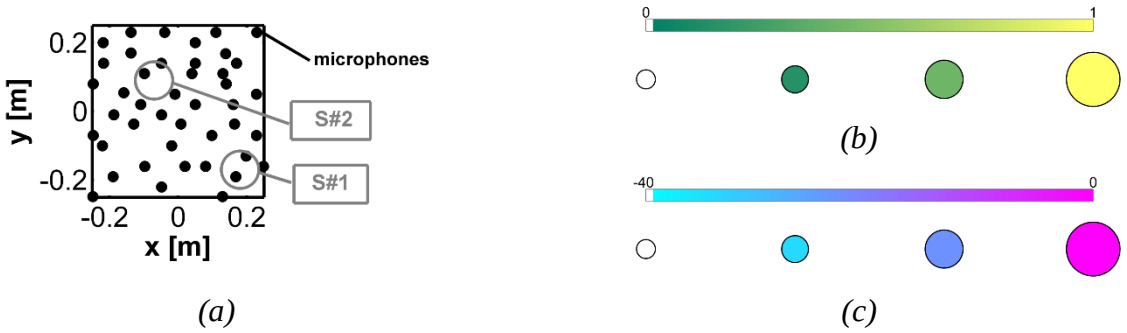

Figure 2: *(a)* 43 randomly distributed microphones array geometry and sources location (0.6 m distance from the array). *(b)* Colour code for the representation of the mask matrix assuming values from 0 to 1. *(c)* Acoustic image (equivalent sources [m^3/s^2]) normalized to the maximum and represented in dB with a dynamic range of 40 dB. In both cases the dots size in the scatter plots is proportional to the represented value.

The clustering mask matrices show local maxima (≈1) in correspondence of the ideal locations of the uncorrelated sources (Fig. 3 *(a)*) – in this case it also allows to separate the acoustic image into two partial contributions – as well as the correlated sources (Fig. 3 *(b)*). The statistical information carried by the mask matrices is consequently exploited to compute the final enhanced acoustic image by placing equivalent sources only in the regions characterized by values of $\gamma^{(i)}$ greater than a wanted threshold (from now on assumed, when not explicitely mentioned, $t_L = 0.5$).

Figure 3: CIB is capable of identifying uncorrelated as well as correlated source distributions, as demonstrated by these result on simulated data. *(a)* Scenario with uncorrelated sources. Example of mask matrices in the 2 kHz 1/3rd octave band. CIB results are reported in Fig. 4 *(a)*. *(b)* Scenario with correlated sources. Example of mask matrix and CIB solution in the 2 kHz 1/3rd octave band.

In the case of uncorrelated sources, S#1 and S#2 partial contributions were successfully separated for all the 1/3rd octave bands studied (Fig. 4 *(a)*). However, in the 1250 Hz third octave band, the S#2 acoustic image shows the effect of a low frequency-related phenomenon of not ideal separation. In that case, in fact, S#1 and S#2 are not separated into two contributions, they appear as a single source placed in between the two ideal locations, instead.

The enhanced acoustic images allow for reliable partial contributions quantification. This is done by comparing the acoustic power of the uncorrelated contributions computed through Eq. (3) with the energetic sum of the equivalent sources distributions identified in the acoustic images through pattern recognition. The interested reader can find the details of the adopted approach in references [9, 11]. The quantification result, for the case of uncorrelated sources adopted in our numerical simulation (Fig. 4 *(b)*), agrees with the theoretical acoustic power frequency content of S#1 and S#2.

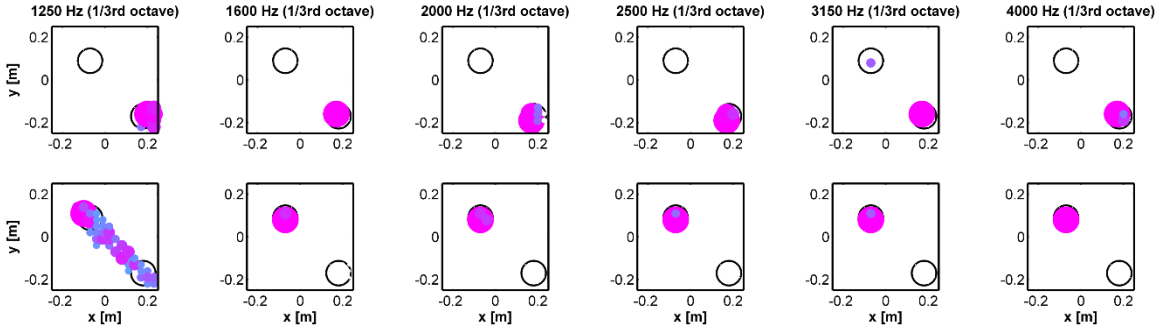

(a)

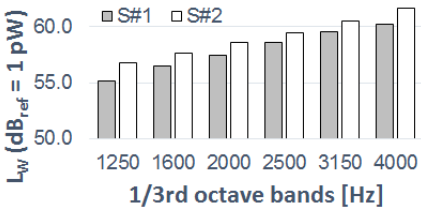

(b)

Figure 4: *(a)* acoustic images of S#1 (above) and S#2 (below) in the case of uncorrelated sources (1/3rd octave frequency band). *(b)* The quantification of the partial contributions of S#1 and S#2 in the case of uncorrelated sources shows that the two sources are indeed identified as white noise sources in the investigated frequency range. It is also correctly found that S#2 strength is systematically greater than S#1's. In the 1250 Hz third octave band, S#2 strength is slightly overestimated because in the lowest frequency lines of that band the two sources are identified as one, located between the two ideal locations of S#1 and S#2.

4. Experimental results on vehicles pass-by noise assessment

The purpose of the example shown below is to prove the capability of CIB in separating uncorrelated acoustic phenomena, ranking the identified sources in terms of radiating acoustic power.

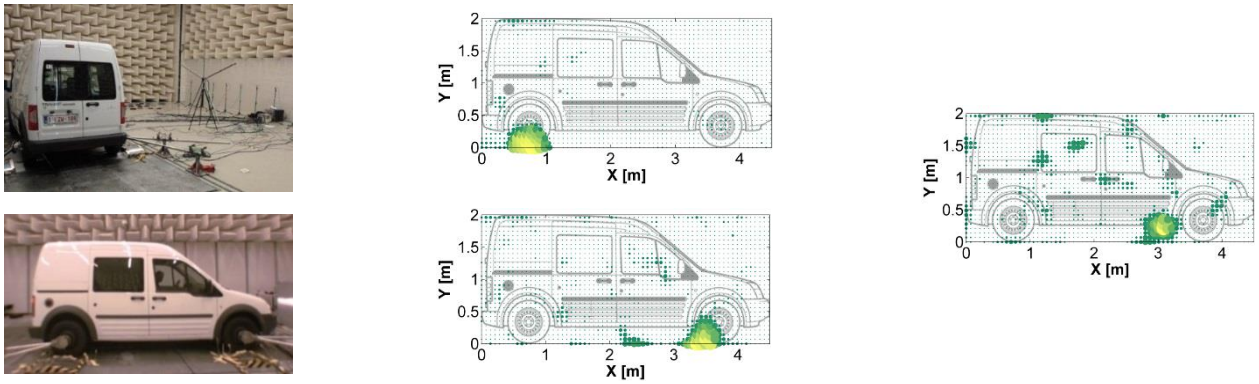

(a) *(b)* *(c)*

Figure 5: Electric vehicle prototype tested in a semi-anechoic room instrumented with a double roller bench for front and rear wheels and a 54 microphones star array for acoustic imaging. *(a)* Vehicle - positioned on the roller bench - in the instrumented room. *(b)* Mask matrices identifying rear and front tire partial contributions (1700 Hz, single frequency line). *(c)* Engine noise contribution is detectable through narrow band analysis (the example refers to 1700 Hz, single frequency line computation, vehicles speed: 50 km/h).

The electric vehicle under test is mounted on a double-drum roller bench capable to move both front and rear wheels, in a semi-anechoic room (Fig. 5 *(a)*). The drums (simulating the contact tire-ground) have been equipped with the configuration "slick" (no road profile was included).

Three main sources are expected to be responsible of the acoustic field generated by the vehicle: front tires, rear tires and noise related to the engine. The three components are supposed to be uncorrelated because related to different causes (in real life front and rear tire noise could be partially correlated because the wheels roll over the same road). In this paper we will focus on tire noise through a broadband 1/3rd octave analysis. The accurate identification of the contribution of the engine would require narrow-band analysis (an example is reported in Fig. 5 *(c)*). Such analysis goes beyond the demonstrative aim of this paper, therefore it was not included in this study.

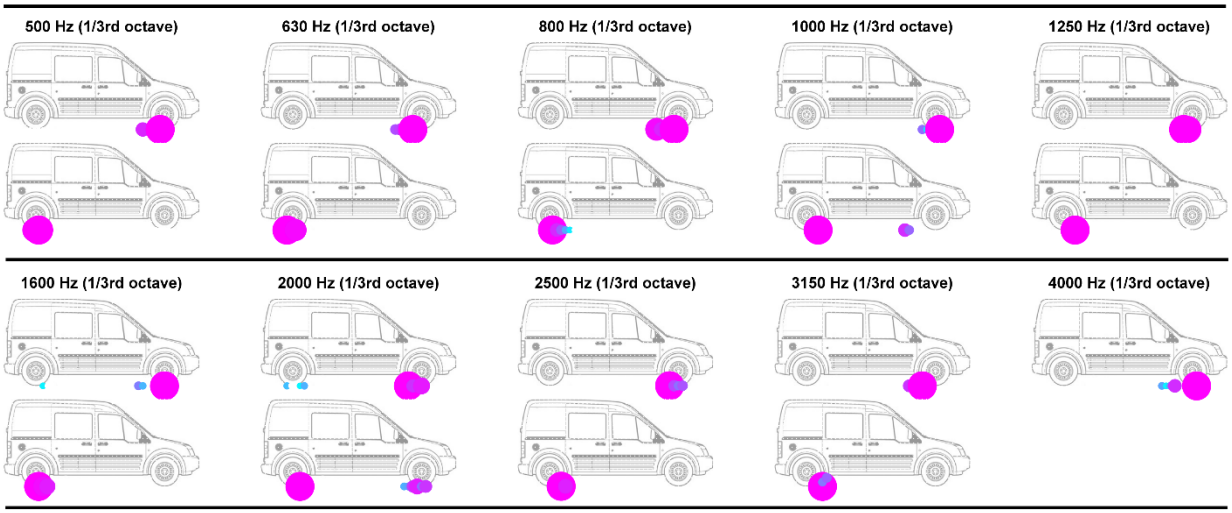

(a)

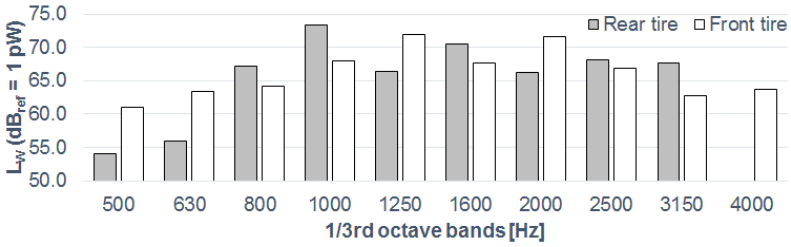

(b)

Figure 6: Vehicle travelling at constant speed (110 km/h). *(a)* Acoustic images of front tire and rear tire per 1/3 octave bands. *(b)* Partial contribution of rear and front tires expressed in terms of acoustic power (L_W, $dB_{ref} = 10^{-12}$ W) and reported per 1/3 octave bands between 500 Hz and 4000 Hz.

The third octave analysis reports the partial contributions of front and rear tires (Fig. 6 *(a-b)*). As expectable, the maximum contribution (in absolute terms) occurs in the 1 kHz 1/3rd octave band. Less obviously, results show that in this latter band the rear tire noise is dominating, while the front tire noise remains prominent in a wider frequency range. In particular, the front tire is the strongest source below 800 Hz, therefore in the low frequency region where tire noise mostly affects the interior of the vehicle.

5. Conclusions

The Clustering Inverse Beamforming algorithm has proved to be a promising frequency domain tool for noise source identification . It has demonstrated to provide high localization accuracy and high dynamic range. The applications on simulated data have shown the capability of CIB in resolving correlated and uncorrelated source distributions, providing partial contribution and absolute quantification. Such tools have been therefore successfully applied on a vehicle tire exterior noise analysis, giving the possibility to separate front and rear tire noise through a third octave analysis. These examples promise CIB to be a powerful tool for vehicles NVH, because it allows advanced analyses

with limited instrumentation and no need of reference sensors. Moreover, the clustering mask matrix entity appears nicely compatible with the concept of "aperture function" adopted in the Bayesian formulation of the ESM problem. This suggest the investigation of further synergies and the extension of CIB towards other ESM approaches.

ACKNOWLEDGEMENTS

This work was supported by the Marie Curie ITN project ENHANCED (joined Experimental and Numerical methods for HumAN CEntered interior noise Design). The project has received funding from the European Union Seventh Framework Programme under grant agreement n° 606800. The whole consortium is gratefully acknowledged.

The e-vehicle measurements on the Ford Transit were carried out in the facilities of IPEK (Karlsruhe Institute of Technology) in the frame of the HEV-NVH research project, which is financially supported by Flemish Institute for Promotion of Innovation (IWT).

REFERENCES

1. Castellini, P., and Sassaroli, A. Acoustic source localization in a reverberant environment by average beamforming. *Mechanical Systems and Signal Processing, **24**(3), 796-808,* (2010).
2. Guidati, S., and Sottek, R. Advanced source localization techniques using microphone arrays. *SAE International Journal of Passenger Cars-Mechanical Systems, **4** (2011-01-1657), 1241-1249,* (2011).
3. Elias, G. Source localization with a two-dimensional focused array: optimal signal processing for a cross-shaped array. *Tiré à part- Office national d'études et de recherches aerospatiales,* (1995).
4. Beguet, B., and Lamotte, L. Device for localizing acoustic sources and measuring their intensities. *U.S. Patent No. 7,903,500. Washington, DC: U.S. Patent and Trademark Office,* (2011).
5. Lamotte, L., Minck, O., Paillasseur, S., Lanslot, J., and Deblauwe, F. Interior Noise Source Identification With Multiple Spherical Arrays In Aircraft And Vehicle. *ICSV 20th, Bangkok, Thailand,* (2013).
6. Antoni, J. A Bayesian approach to sound source reconstruction: optimal basis, regularization, and focusing The Journal of the Acoustical Society of America, 131, 2873-2890. (2012).
7. Colangeli, C., Chiariotti, P., Janssens, K., and Castellini, P.. A microphone clustering approach for improved Generalized Inverse Beamforming formulation. *In INTER-NOISE and NOISE-CON Congress and Conference Proceedings (Vol. 251, No. 1, pp. 770-780). Institute of Noise Control Engineering,* (2015).
8. Colangeli, C.; Chiariotti, P.; Battista, G.; Castellini, P. and Janssens, K. Clustering inverse beamforming for interior sound source localization application to a car cabin mock-up. *In the proceedings of the Berlin Beamforming Conference,* (2016).
9. Colangeli, C. Clustering Inverse Beamforming and multi-domain acoustic imaging approaches for vehicles NVH. *Ph.D. thesis. Università Politecnica delle Marche,* (2017).
10. Suzuki, T. L1 generalized inverse beam-forming algorithm resolving coherent/incoherent, distributed and multipole sources. *Journal of Sound and Vibration, 330(24), 5835-5851,* (2011).
11. Colangeli, C., Chiariotti, P., and Janssens, K. Uncorrelated noise sources separation using inverse beamforming. *In Experimental Techniques, Rotating Machinery, and Acoustics, Volume 8 (pp. 59-70). Springer International Publishing,* (2015).
12. Hansen, P. C. Regularization tools: A Matlab package for analysis and solution of discrete ill-posed problems. *Numerical algorithms, Springer, 6, 1-35,* (1994).